

Millisecond-range electron spin memory in singly-charged InP quantum dots

Bipul Pal,^{1,*} Michio Ikezawa,¹ Yasuaki Masumoto,¹ and Ivan V. Ignatiev^{1,2}

¹*Institute of Physics, University of Tsukuba, Tsukuba 305-8571, Japan*

²*Institute of Physics, St. Petersburg State University, St.-Petersburg 198504, Russia*

(Dated: May 10, 2019)

We report millisecond-range spin memory of resident electrons in an ensemble of InP quantum dots (QDs) under a small magnetic field of 0.1 T applied along the optical excitation axis at temperatures up to about 5 K. A pump-probe photoluminescence (PL) technique is used for optical orientation of electron spins by the pump pulses and for study of spin relaxation over the long time scale by measuring the degree of circular polarization of the probe PL as a function of pump-probe delay. Dependence of spin decay rate on magnetic field and temperature suggests two-phonon processes as the dominant spin relaxation mechanism in this QDs at low temperatures.

PACS numbers: 78.67.Hc, 78.55.Cr, 78.47.+p, 72.25.Rb

Electron spin in semiconductors may be suitable for use as a quantum memory in quantum repeaters as semiconductors are capable of converting photons to electrons (and holes) while transferring quantum information from photon polarization to electron spin, and vice versa.¹ However, a long spin relaxation time (τ_s) is necessary to realize spin quantum memory. In semiconductor quantum dots (QDs) τ_s up to a few ms was theoretically predicted as a result of suppression of important spin relaxation mechanisms due to 3D confinement and lack of energy dispersion.^{2,3,4} This has stimulated experimental investigations of long spin memory in QDs.^{5,6,7,8,9,10,11} For example, electron spin relaxation time of about 200 μ s in InGaAs vertical QDs⁶ at $T \leq 0.5$ K and zero external magnetic field (B), about 0.85 ms in electrically gated GaAs lateral QDs⁷ at $T < 0.3$ K and $B = 8$ T, and about 20 ms in self-assembled InGaAs QDs⁸ at $T = 1$ K and $B = 4$ T has been recently reported. Many of the previous results of long spin memory in QDs were obtained in InGaAs and GaAs QDs under special condition of low temperature (≤ 1 K) and large magnetic field (≥ 4 T).

In this letter we report observation of optically created electron spin-orientation surviving up to about 1 ms in an ensemble of singly negatively charged InP QDs at $B = 0.1$ T applied along the optical excitation axis at $T \sim 5$ K. The sample consists of a single layer of self-assembled InP QDs embedded between GaInP barriers. The average base diameter (height) of the QDs is about 40 (5) nm with an areal density $\sim 10^{10}$ cm⁻². We use a pump-probe PL technique^{5,10,11} to study electron spin orientation dynamics by measuring the circular polarization [defined as $P = (I^{++} - I^{+-})/(I^{++} + I^{+-})$, where $I^{++(-)}$ is the PL intensity for excitation with σ^+ probe and detection of $\sigma^{+(-)}$ probe PL] of the probe pulse PL in presence of a preexcitation by a pump pulse. Our experimental setup is schematically shown in Fig. 1(a).

A CW Ti:sapphire laser beam is split into pump and probe beams. Two acousto-optic modulators (AOM) driven by programmable function generator (PFG) generates pump and probe pulses with controllable pulse width and delay (τ) between them. Glan-Thompson polarizers (GTP) and wave plates are used to control

the circular polarization of the pump and probe beams. The PL signal is sent through a combination of a photoelastic modulator (PEM) and a GTP before dispersing in a monochromator and detecting in a GaAs photomultiplier tube (PMT). The PMT output is connected to a two-channel gated photon counter (GPC). The PEM acts as an oscillating $\lambda/4$ -plate and when combined with GTP, allows detection of PL intensity in the σ^+ and σ^- channels. The PEM frequency, $f_P = 42$ kHz, is reduced to $f_T = f_P/(n + 0.5)$ (typically $n = 40$ in our measurements) to trigger the PFG and GPC.¹² Thus, one probe pulse (and A-gate of the GPC) is centered at the $+\lambda/4$ and the next probe pulse (and B-gate of the GPC) is centered at the $-\lambda/4$ retardation peaks of the PEM [Fig. 1(b)]. We typically use a GPC gate width of 5 μ s, while the pump (probe) pulse width is 60 (3) μ s, giving a pump (probe) power density [$W_{\text{pump (probe)}}$] of about 0.5 (0.05) W cm⁻². The low probe power density ensures that the pump-induced spin polarization is not fully erased by the probe pulse. The excitation energy is tuned to about 1.771 eV (below-barrier, QD excited state excitation) and the QD ground state PL is detected at about 1.729 eV. An external electric bias of $U_{\text{bias}} = -0.1$ V is applied to the sample. We find that under this condition the PL polarization is negative and reaches maximum.¹¹ A study of trionic quantum beats in this sample¹³ showed that at $U_{\text{bias}} \approx -0.1$ V each QD contains one resident electron on an average. This suggests that the negative PL polarization arises from trionic state, as is discussed e.g., in Refs. 5,9,14,15.

In our experiments, a σ^+ (or σ^-) polarized pump induces \downarrow (or \uparrow) spin orientation of the resident electrons.¹⁶ A probe pulse, variably delayed with respect to the pump pulse, tests this pump-induced spin-orientation. The probe beam (always σ^+ polarized) creates a hot trion with *parallel* [$\downarrow\downarrow$ -QDs] or *anti-parallel* [$\uparrow\downarrow$ -QDs] electron spins. After a flip-flop process in $\downarrow\downarrow$ -QDs shown schematically in Fig. 2(a), the probe PL polarization becomes negative,¹¹ while it is positive for the $\uparrow\downarrow$ -QDs [Fig. 2(b)]. At any given τ the net probe PL polarization is determined by the ratio of $\downarrow\downarrow$ - and $\uparrow\downarrow$ -QDs.

We measure the probe PL polarization for (i) co-

circularly polarized pump-probe (P_{CO}) [pump creates more $\downarrow\downarrow$ -QDs] and (ii) cross-circularly polarized pump-probe (P_{CR}) [pump creates more $\uparrow\downarrow$ -QDs] [pump and probe polarizations for the two cases are indicated in Fig. 1(b)]. A small static magnetic field of $B = 0.1$ T is applied parallel to the optical excitation (and sample growth) axis to suppress the effect of fluctuating nuclear magnetic field.^{18,19} Polarizations P_{CR} and P_{CO} as a function of τ are shown in Fig. 2(c). The difference $P_{CR} - P_{CO}$ is a good measure of the pump induced spin orientation of the resident electrons.²⁰ A semilogarithmic plot of $P_{CR} - P_{CO}$ obtained from Fig. 2(c) shows that the spin memory decay is nonexponential [Fig. 2(d)]. Thus, a spin relaxation time cannot be defined in a simple way. However, it is clear from this data that the spin memory decays on a millisecond time-scale.

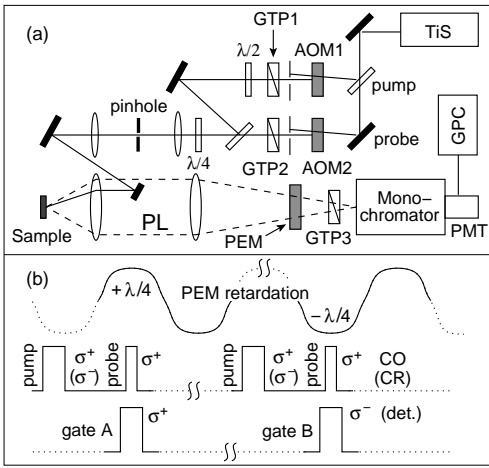


FIG. 1: Schematic of the experimental setup (a) and time synchronization (b) of the PEM retardation, the probe pulses, and the GPC gates.

The observed long-lived spin polarization could result from a dynamic nuclear polarization which may appear under the experimental condition used.^{17,18,21} However, in a recent study¹¹ of this aspect we have shown that very small effective magnetic field (< 0.02 T) in InP QDs,^{22,23} arising from dynamic nuclear polarization, is not consistent with the large amplitude of PL polarization observed in this sample. Thus, the long spin memory observed here should be related to the lack of efficient spin decay path in QDs. To investigate the spin relaxation mechanisms effective in this case we study temperature and magnetic field dependence of the spin decay process.

Figure 3 shows decay of $P_{CR} - P_{CO}$ at a few temperatures for $B = 0.1$ T. A faster decay is seen with increasing T . As noted earlier, the decay is nonexponential and suggests a distribution of decay rates, which may arise due to inhomogeneous environment and size-distribution of the QDs.¹¹ Theoretical analysis shows (see e.g., Ref. 24) that a spread of the relaxation rate results in a nonexponential decay of the form $\sim \exp[-(\gamma_s \tau)^c]$ (the so-called stretched exponential function), where the parameter c

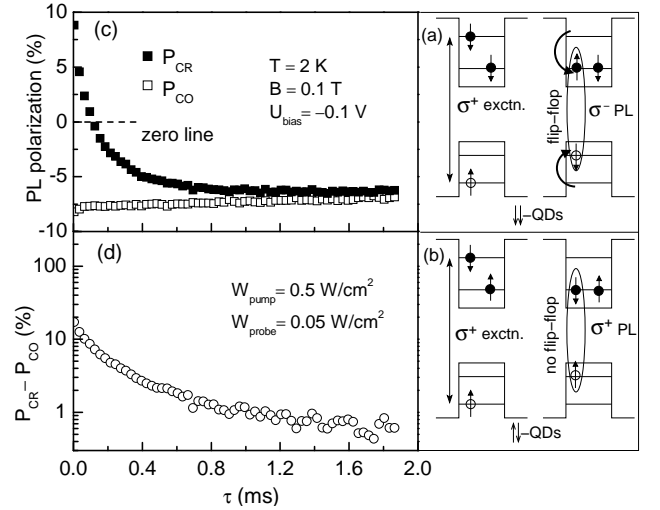


FIG. 2: Schematics of $\downarrow\downarrow$ -QDs (a) and $\uparrow\downarrow$ -QDs (b). Probe PL polarization for co- (P_{CO}) and cross- (P_{CR}) circularly polarized pump-probe (c), and the difference $P_{CR} - P_{CO}$ (d) as a function of τ .

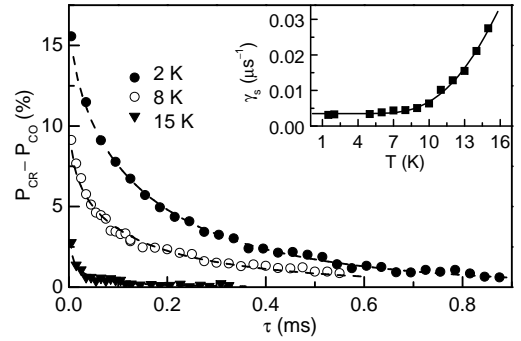


FIG. 3: Delay dependence of $P_{CR} - P_{CO}$ at a few T . $B = 0.1$ T, $U_{bias} = -0.1$ V, $W_{pump (probe)} = 0.5 (0.05)$ W cm⁻². Dashed lines are stretched exponential fits (discussed in the text). Inset shows spin decay rate (γ_s) as a function of T .

depends on the physical processes causing the spread. We find that the function fits our data very well (dashed lines in Fig. 3) if we use c as a fitting parameter. Effective spin decay rate γ_s obtained from such fits is plotted in the inset of Fig. 3 as a function of T . A rapid increase in γ_s is seen for $T > 8$ K. Such an increase is expected for thermally activated spin relaxation due to the phonon-mediated coupling of the ground and excited electron states (two-phonon Orbach process).²⁵ We find that the function $\gamma_s \sim (\exp[\Delta E/k_B T] - 1)^{-1} + \gamma_0$ ($\Delta E =$ activation energy, $k_B =$ Boltzmann constant, and γ_0 stands for spin decay rate arising from temperature independent relaxation mechanisms) describing this process fits the data very well (solid line in the inset of Fig. 3). From the fit we obtain $\Delta E \approx 5$ meV. This value is smaller than that obtained experimentally for electron level spacing of 15 meV in Ref. 13. This discrepancy is probably due to the difference in QD sub-ensemble probed in the two cases.

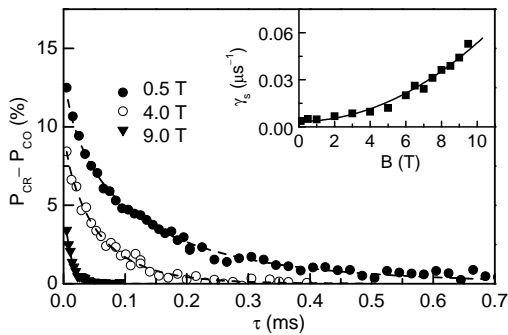


FIG. 4: Delay dependence of $P_{CR} - P_{CO}$ at a few B . $T = 2$ K, $U_{bias} = -0.1$ V, $W_{pump} (probe) = 0.5$ (0.05) $W\text{ cm}^{-2}$. Dashed lines are stretched exponential fits (discussed in the text). Inset shows spin decay rate (γ_s) as a function of B .

We now present the magnetic field dependence of the spin decay process. Decay of $P_{CR} - P_{CO}$ at a few values of B at $T = 2$ K is shown in Fig. 4. We find that the decay becomes increasingly faster with increase in B . An effective spin decay rate obtained from stretched exponential fit to the data is plotted as a function of B in the inset of Fig. 4. Decay rate γ_s is found to increase superlinearly with B . Several possible mechanisms for such an increase are discussed in the literature.^{3,4,26} Magnetic field couples the higher energy states with nonzero orbital momentum to the electron spin states split by the magnetic field (Zeeman splitting) that allows a small admixture of the states of opposite spin to each Zeeman sublevel.^{3,4} At low temperature this enables spin-flip transition between Zeeman sublevels via participation of acoustic phonons to dissipate energy (one-phonon resonant process). With increasing B the Zeeman splitting increases. Due to higher density of resonant phonons at increased energy

and more efficient mixture of the states by the magnetic field, the spin relaxation rate increases. Theoretical calculations^{3,4} have predicted $\gamma_s \sim B^5$ at very low temperature and large magnetic field if the spin-orbit interaction and the one-phonon scattering dominate. However, for T of about a few kelvin, the two-phonon nonresonant (Raman) scattering may become important.⁴ In that case, the magnetic field dependence is only determined by the admixture of the excited states and becomes quadratic.³ Our data in Fig. 4-inset can be fitted very well with $\gamma_s = \alpha + \beta B^2$. This argues for the two-phonon scattering as the main mechanism of acceleration of the spin relaxation in magnetic field.

The acceleration of spin relaxation could also result from hyperfine interaction.²⁶ However, this is unlikely in our case due to very small nuclear spin polarization in the InP QDs^{22,23} we studied.

In conclusion, we have observed long spin memory, persisting over 1 ms, in an ensemble of singly negatively charged InP QDs at small magnetic field (0.1 T) and at moderate temperature (~ 5 K). Our data on the magnetic field and temperature dependence of spin decay rate suggests two-phonon scattering may be the dominant spin relaxation mechanism. Long spin memory observed here in III-V semiconductor QDs is relevant for quantum information communication and storage. Though our study is made at about $0.7\ \mu\text{m}$ wavelength (λ), III-V semiconductor system can be easily adapted to $\lambda = 1.3$ and $1.5\ \mu\text{m}$, suitable for fiber optic communication.

Authors thank I. Ya. Gerlovin and T. Takagahara for fruitful discussions. B. Pal thanks INOUE Foundation for Science, Japan, for financial support. This work is supported by the Grant-in-Aid for the Scientific Research #13852003 and #16031203 from the MEXT, Japan.

* E-mail: bipulpal@sakura.cc.tsukuba.ac.jp
¹ D. D. Awschalom *et al.*, *Semiconductor Spintronics and Quantum Computation*, (Springer-Verlag, Berlin 2002).
² V. Khaetskii *et al.*, Phys. Rev. B **61**, 12639 (2000).
³ A. V. Khaetskii *et al.*, Phys. Rev. B **64**, 125316 (2001).
⁴ L. M. Woods *et al.*, Phys. Rev. B **66**, 161318 (2002).
⁵ S. Cortez *et al.*, Phys. Rev. Lett. **89**, 207401 (2002).
⁶ T. Fujisawa *et al.*, Nature **419**, 278 (2002).
⁷ J. M. Elzerman *et al.*, Nature **430**, 431 (2004).
⁸ M. Kroutvar *et al.*, Nature **432**, 81 (2004).
⁹ S. Laurent *et al.*, Physica E **20**, 404 (2004).
¹⁰ J. S. Colton *et al.*, Phys. Rev. B **69**, 121307(R) (2004).
¹¹ M. Ikezawa *et al.*, Phys. Rev. B (to be published).
¹² V. K. Kalevich *et al.*, Instrum. Exp. Techn. **21**, 199 (1978).
¹³ I. E. Kozin *et al.*, Phys. Rev. B **65**, 241312(R) (2002).
¹⁴ K. V. Kavokin, Phys. Status Solidi (a) **195**, 592 (2003).
¹⁵ A. S. Bracker *et al.*, Phys. Rev. Lett. **94**, 047402 (2005).
¹⁶ Various mechanisms of optical orientation of spins are discussed e.g., in Refs. 5,15,17. Possible mechanisms of optical orientation of resident electron spins in InP QDs under study will be discussed elsewhere.

¹⁷ F. Meier and B. P. Zakharchenya, *Optical Orientation* (North-Holland, Amsterdam, 1984).
¹⁸ I. A. Merkulov *et al.*, Phys. Rev. B **65**, 205309 (2002).
¹⁹ P.-F. Braun *et al.*, Phys. Rev. Lett. **94**, 116601 (2005).
²⁰ Effect of dynamic nuclear polarization (if present) is expected to be the same for P_{CR} and P_{CO} and taking their difference may eliminate the influence of dynamic nuclear polarization in the range of our measurement. A direct relation between $P_{CR} - P_{CO}$ and the spin-orientation of resident electrons will be discussed elsewhere.
²¹ D. Gammon *et al.*, Phys. Rev. Lett. **86**, 5176 (2001).
²² I. V. Ignatiev *et al.*, Proc. 13th Int. Symp. Nanostructures: Physics and Technology, St. Petersburg, Russia, 2005; also available on-line at lanl.arXiv.org: cond-mat/0508698.
²³ R. I. Dzhioev *et al.*, Phys. Solid State **41**, 2014 (1999).
²⁴ R. Chen, J. Lumin. **102-103**, 510 (2003) and Refs. therein.
²⁵ A. Abragam and B. Bleaney, *Electron Paramagnetic Resonance of Transition Ions*, (Clarendon Press, Oxford, 1970).
²⁶ S. I. Erlingsson *et al.*, Phys. Rev. B **66**, 155327 (2002).